Modeling of Particle Bonding in Cold Spray

S. Muftu[1], A. Gouldstone[1], M. Upmanyu[1], T. Ando[1],
S. A. Alavian[2], A. Hulton[2], B. Yildirim[2]

Northeastern University
Department of Mechanical Engineering
Boston, MA 02115

[2]Former graduate students, [1]Professors

Acknowledgements

- The National Science Foundation, Grant number 1130027
- H.C. Stark, Inc. (Newton, MA)
- Plasma Giken, Co. Ltd. (Tokyo, Japan)

Past work at NU related to modeling and simulations of Cold Spray particle impact phenomenon

- FE modeling approaches for CS (1, 5)
- Models of particle adhesion (1, 3 – 6)
- Assessment of interface energy (3, 4)
- Multi-particle impact and cohesion (5, 6)
- **Effects of particle and substrate temperatures and effects of impact frequency (6)**
- Molecular dynamics simulation of impact (in preparation)

References

1. B. Yildirim, S. Müftü, A. Gouldstone, "**Modeling of High Velocity Impact of Spherical Particles**," *Wear*, Vol. 270(9-10), pp. 703-713, 2011.
2. B. Yildirim, S. Müftü, "**Impact of High Velocity Particles onto a Rough Surface**," *International Journal of Solids and Structures*, Vol. 49, pp. 1375-1386, 2012.
3. Yildirim, H. Fukanuma, T. Ando, A. Gouldstone and S. Müftü, "**A numerical investigation into cold spray bonding processes**," *Journal of Tribology*, Vol. 137, No. 1, pp. 935-942, 2014.
4. S. Müftü, S. Zhalehpour, A. Gouldstone, and T. Ando, "**Assessment of Interface Energy in High Velocity Particle Impacts**" Proceedings of the *38th Annual Meeting, The Adhesion Society February 20-25, 2015, Savannah, GA*
5. B. Yildirim, ***Mechanistic modeling of high velocity micro-particle impacts: Application to material deposition by cold spray process*** **,** PhD Thesis, Northeastern University, April 11**,** 2013
6. A. Hulton, ***Investigation of the Effects of Particle Temperature and Spacing on Multiparticle Impacts in Cold Spray***, MS Thesis, Northeastern University, August 2013

Goals – initially morphology-based

Investigate the effects of

- Thermal state of the particles and the substrate, and
- Spatial and temporal spacing of the particles in **multi-particle impacts** in cold spray

Modeling Considerations

- Material model
- Gas-particle flow
- Time between impacts and thermal response of the impacted particle/substrate

Synergistic Activities

- Experimental analysis of interfaces
- MD simulations

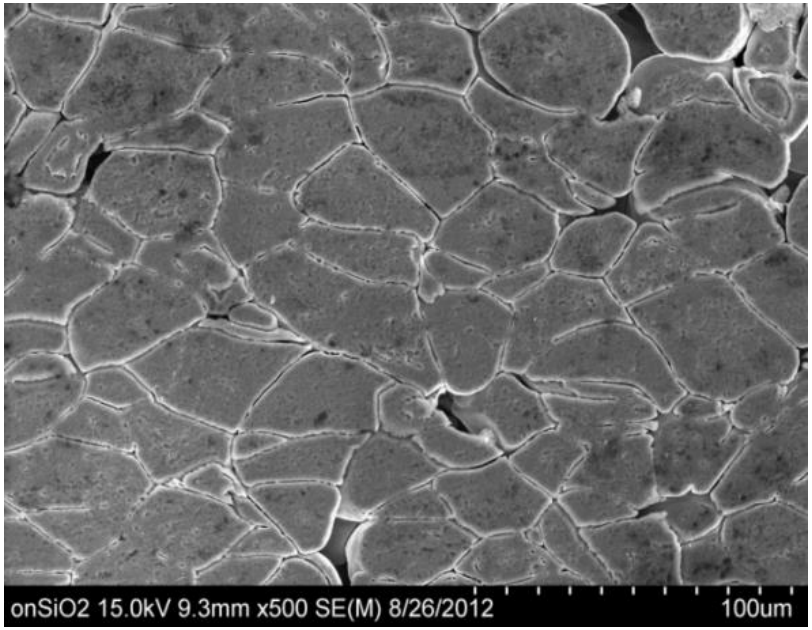

SEM image (Ali Alavian)

- Al particles on Al substrate
- 573 K gas inlet temperature

[1] P. Fauchais and G. Montavon, "Thermal and cold spray: Recent developments," *Key Engineering Materials,* vol. 384, pp. 1-59, 2008.
[2] H. Assadi et al., "Bonding mechanism in cold gas spraying," *Acta Materialia,* vol. 51, pp. 4379-4394, 2003.

Gas-Particle Interaction (for multi-particle impact)

- Provided with gas T (no inflight diagnostics)
- We developed our own 1D Code
- 1D particle-gas flow model [7]
  - Isentropic
  - Compressible gas flow
  - Interactions between particles are neglected
- Determine particle velocity and temperature at impact

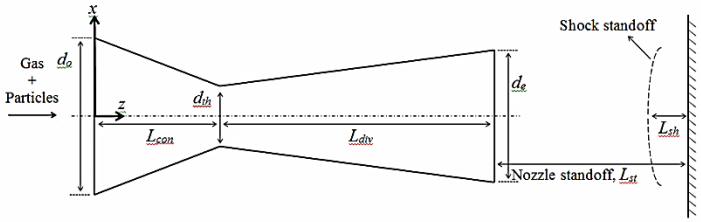

Par	Sub	Gas T (K)	Par V (m/s)	Par T (K)
Al	Al	773	677	602
Al	Al	673	632	525
Al	Al	573	581	449

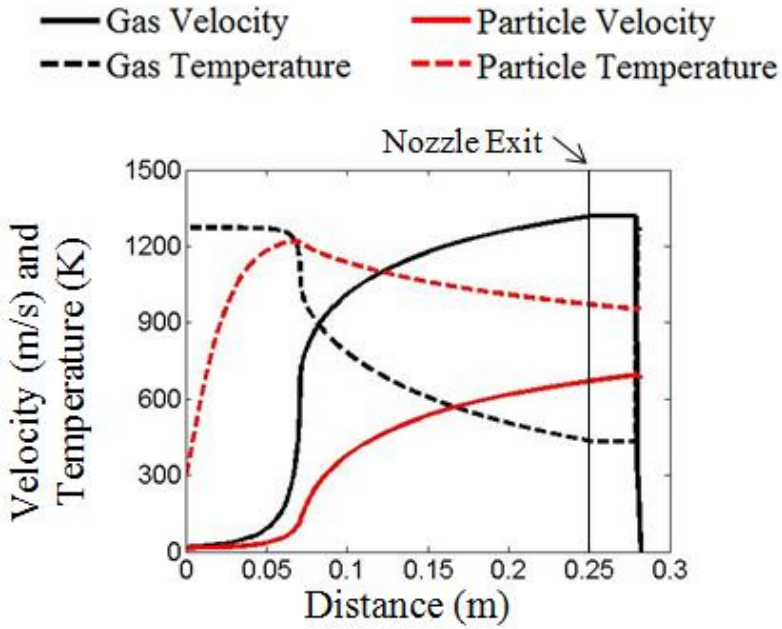

[7] R. C. Dykhuizen and M. F. Smith, "Gas dynamic principles of cold spray," *Journal of Thermal Spray Technology,* vol. 7, pp. 205-212, 1998.
[8] Results obtained via ParticleFlowSim

Average time between impacts

t_{ave} = (No. of impacting particles)/ (No. of Particles/unit time)

$$t_{ave} = \left(\frac{A_e}{A_d}\right)\left(\frac{m_p}{f_p}\right)$$

$$t_{ave} = \left(\frac{m_p}{f_p}\right)\left(\frac{A_e}{A_d}\right) = \frac{\frac{4}{3}\pi\rho_p\left(\frac{1}{2}d_p\right)^3}{f_p}\frac{A_e}{4\pi\left(\frac{1}{2}d_p\right)^2} = \frac{\rho_p d_p A_e}{6 f_p}$$

m_p : mass density of particles (mass/vol)
d_p : diameter of particles (length)
A_e : Nozzle exit area (area)
f_p : Particle feed rate (mass/time)

t_{ave} ~ 100 ms estimated average time between impacts at the same position (no raster)

m_p : 8900 kg/m3
d_p : 25 µm
d_e : 6.5 mm
f_p : 0.01 kg/s

Material Model

- Johnson Cook plasticity model
  - Temperature
  - Strain
  - Strain rate
  - Material constants *A, B, C, n, m,* and T_m
- Plastic work converted to heat
  - β = 0.9 (90% of strain energy is converted to heat)

- Stress Based Cohesion Model
  Fraction of material yield stress
  - Oxide, impurities

$$\sigma_y(\varepsilon_{\mathrm{p}}, \dot{\varepsilon}_{\mathrm{p}}, T) = [A + B(\varepsilon_{\mathrm{p}})^n]\,[1 + C\ln(\dot{\varepsilon}_{\mathrm{p}}{}^*)]\,[1 - (T^*)^m]$$

$$\dot{\varepsilon}_{\mathrm{p}}{}^* := \frac{\dot{\varepsilon}_{\mathrm{p}}}{\dot{\varepsilon}_{\mathrm{p0}}} \quad \text{and} \quad T^* := \frac{(T - T_0)}{(T_m - T_0)}$$

- Shear material failure
  - Relationship between Johnson-Cook model and shear instability strain
  - Produces maximum plastic strain at which material fails
  - Equivalent plastic strain ε_p = 2

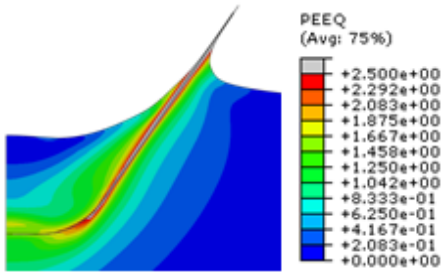

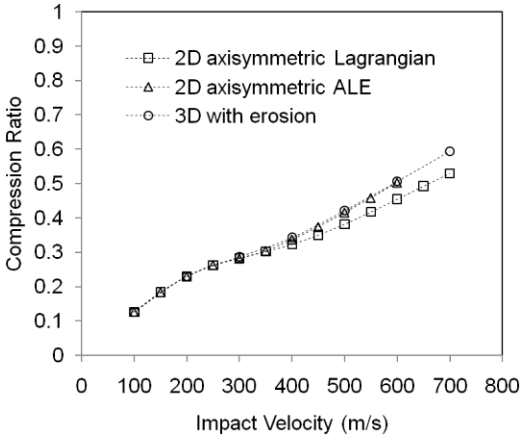

[5] An et al. "Mechanical Behavior of Solder Joints Under Dynamic Four Point Impact Bending ", Microelectronics Reliability 51 2011, 1011-1019

Typical Run

- Model input parameters
  - Particle velocity and temperature
  - Substrate temperature
  - Par/Sub material properties
    - *E, ρ, v, α, k*

- Symmetrical impact of 3 particles
- Horizontal spacing of impacts
- Substrate heating due to gas
- Particle impact frequency (flow-rate)

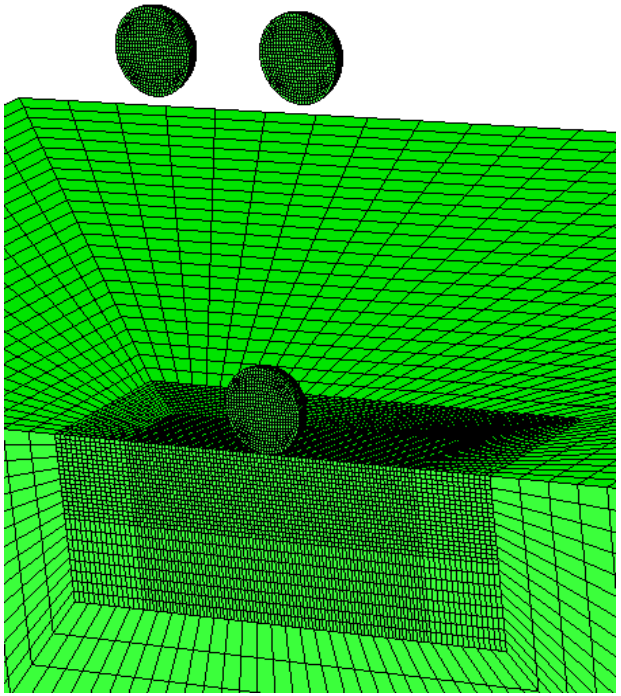

Heating of the Substrate, T_s

- Effect of substrate temperature
  - Accounting for substrate temperature results in higher T_s
- Less initial particle deformation
  - More deformation in substrate
    - Softer material absorbs more energy

$V_i^{(p)}$ = 677 m/s, $T_i^{(p)}$ = 602 K

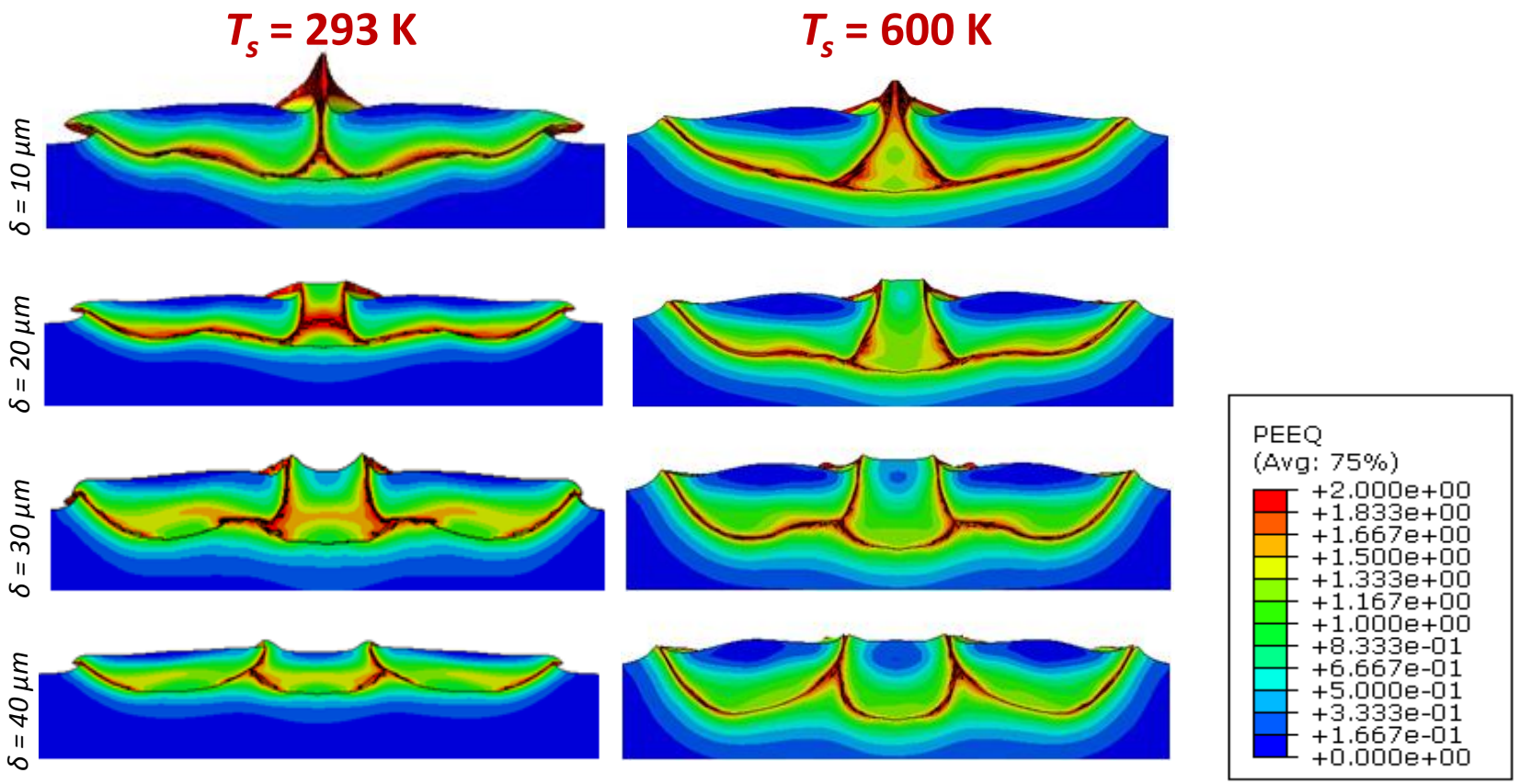

Material: Aluminum D_p = 31 μm

Impact frequency (mass flowrate)

- Simulated by cooling the initial particle
  - Less deformation in the initial particle
    - More pronounced for smaller δ

$V_i^{(p)}$ = 677 m/s, $T_i^{(p)}$ = 602 K, T_s = 600 K

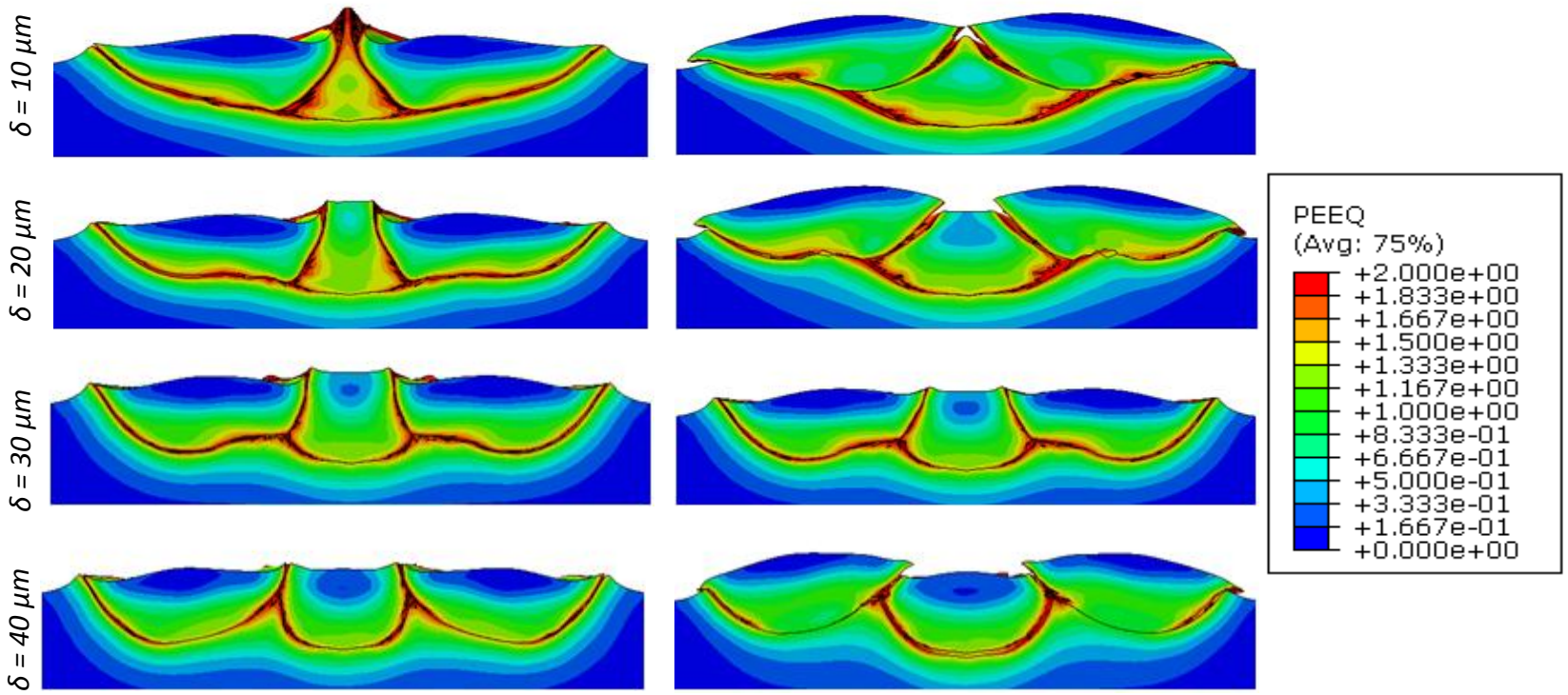

With hot initial particle | With cooled initial particle

Material: Aluminum D_p = 31 μm T_s = 600 K

Shape metrics to provide quantitative measure of deformation

- Axis Ratio
  - Max/Min of ellipse axes
- Eccentricity
  - Circularity of object
  - Circle=1 while line→∞
- Equivalent Diameter
  - Diameter of circle with same area
- Orientation angle
  - Angle of major ellipse axis

- Perimeter
- Elongation
  - $EL = \log_2(a/b)$
  - a, b are ellipse major and minor axes
- Dispersion
  - $DP = \log_2(\pi ab)$
  - Ellipse=0 and increases with roughness
- Roundness
  - $RN = P^2/4\pi A$
  - Circle=1 while line→∞

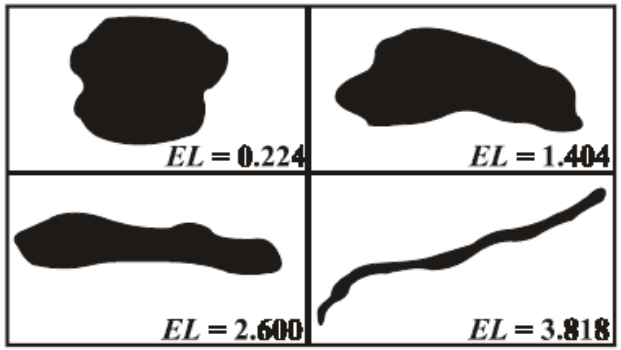

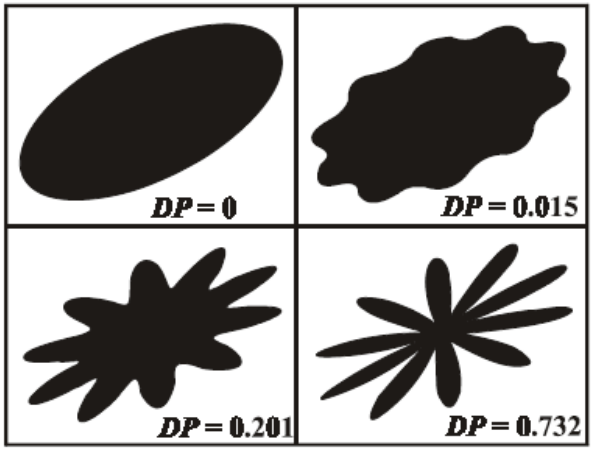

MIKLI, V., KÄERDI, H., KULU, P., BESTERCI, M. Characterization of Powder Morphology. Proc. Estonian Acad. Sci. Eng., 2001, **7**, 1, 22–34

Experimental Considerations

Metallography of aluminum cold-sprayed samples

Powder	Substrate	Spray condition
Al	A5052	N_2, 3MPa, 573K
		N_2, 3MPa, 673K
		N_2, 3MPa, 773K

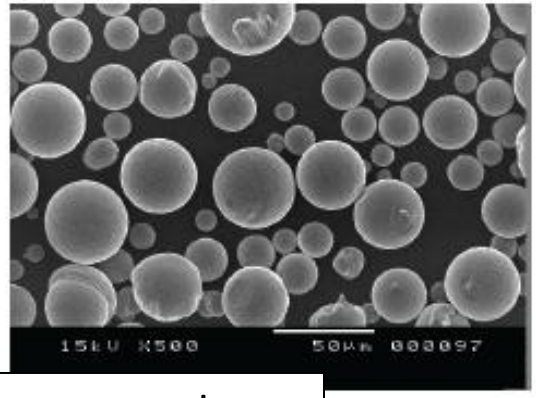

Aluminum powder
Volume average: 35 µm
Number average: 27 µm

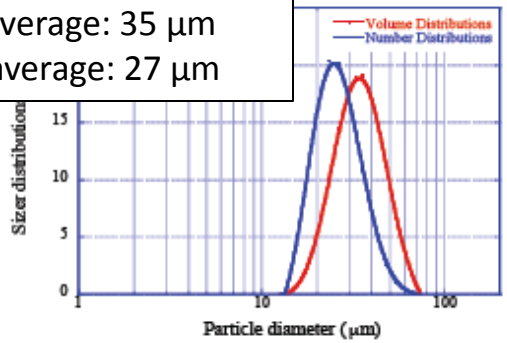

Sample preparation:

- Samples cut into 1 × 0.5 cm
- Mechanically grinded and polished to 0.3 µm
- Chemically etched (see Table)
- Microstructures studied with Hitachi S4800 field-emission SEM

Coat	Etchant	Concentration	Time
Al	Distilled water	95 ml	30 s
	Hydrochloric acid	1.5 ml	
	Nitric acid	2.5 ml	
	Hydrofluoric acid	1 ml	

- All samples supplied by Plasma-Giken

Heterogeneous Bonding in Al Samples

573K

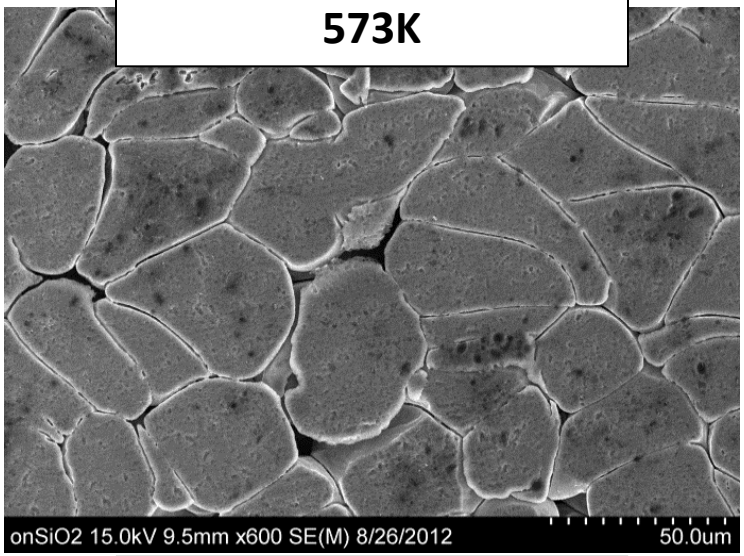

673K

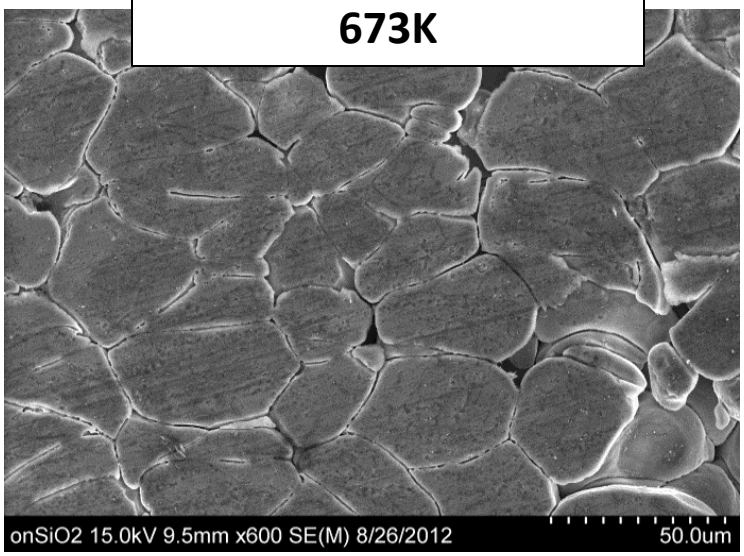

773K

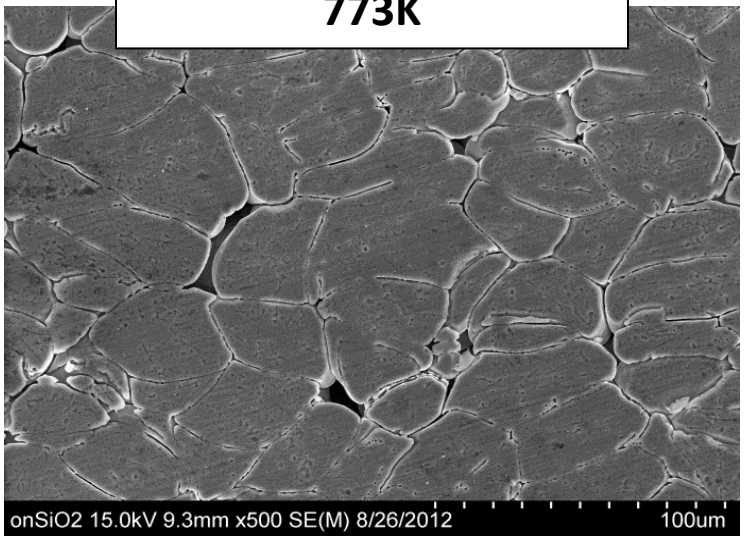

- Key feature: Heterogeneous etching of interfaces
  - Deposition Temperature-Dependent
    - Spacing/Pitch (O) tens of microns

Different types of interfaces in etched Aluminum samples

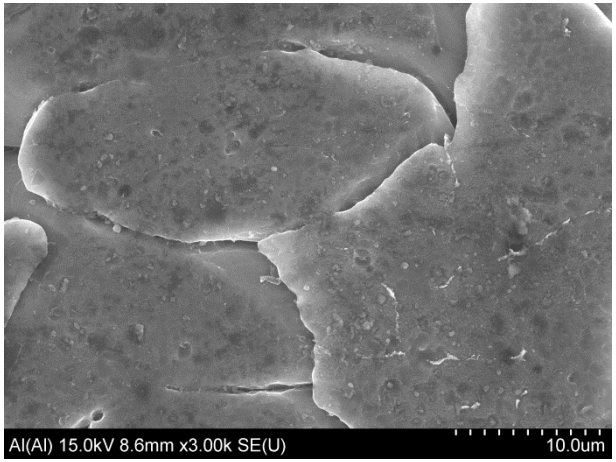

Aluminum on A5052 (573K)

Aluminum on A5052 (673K)

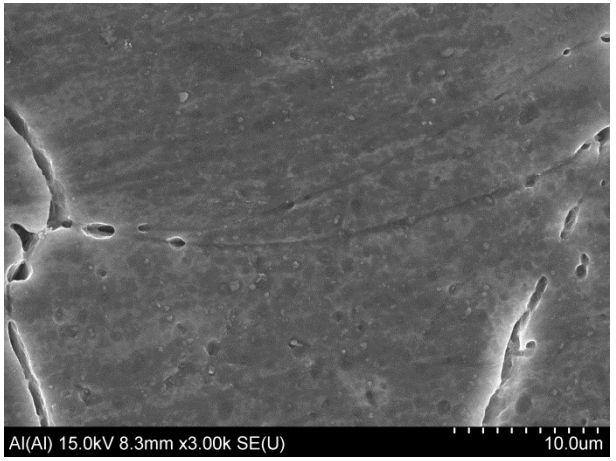

Aluminum on A5052 (673K)

1. Interfaces that are removed by etching solution completely.
2. Interfaces that removed by etching solution partially and some holes form at the interface.
3. Interfaces that are not removed by etching solution.

Reaction initiated from trapped oxide particle in the form of isolated holes

Why different behavior at interface?

Effect of Hydrostatic pressure on etching rate:

- In cold spray process we are not dealing with uniaxial stress field like the experiment done by Sarkar-Aquino. So it is more convenient to examine the effect of hydrostatic pressure on etching rate.
- In the figure changes of aluminum reaction rate with acid are calculated for a range of pressure fields.
- Aluminum atomic volume is about 10 cm^3/mole and pressure can have large effect on its reaction rate.

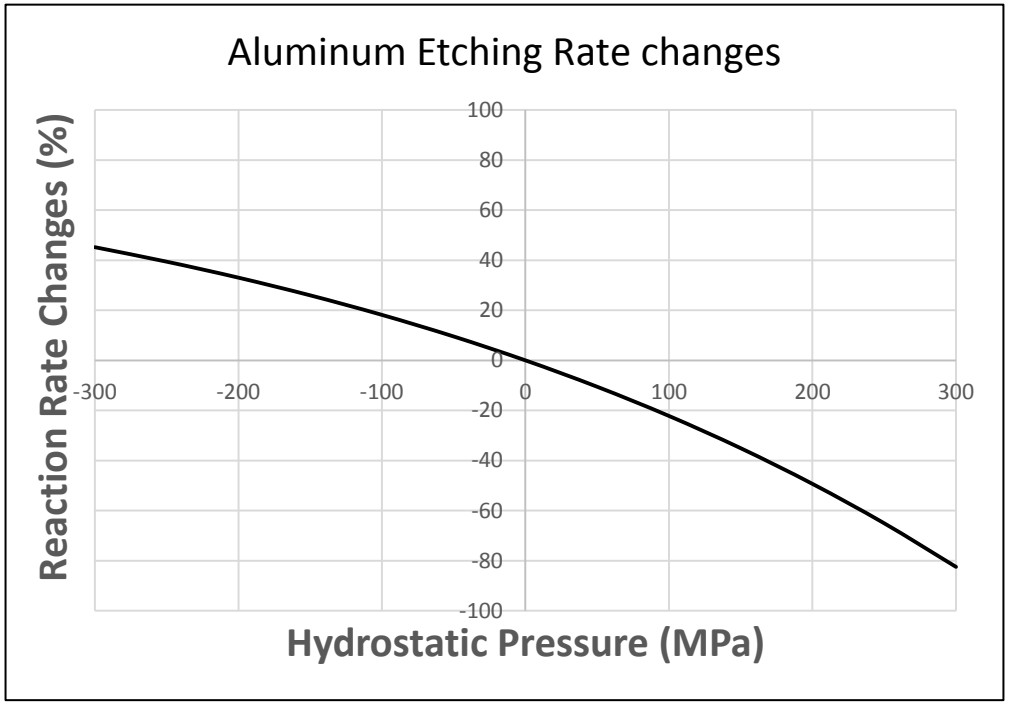

* Swarnavo Sarkar, Wilkins Aquino, Changes in electrodic reaction rates due to elastic stress and stress-induced surface patterns, Electrochimica Acta, Volume 111, 30 November 2013, Pages 814-822,,

Previous Impact model:

- Impact of spherical particle along the Y-axis to the semi-infinite substrate.
- Model type: Dynamic, Temp-displacement, explicit.
- Material properties: **Al1100H12** properties for particle and substrate.

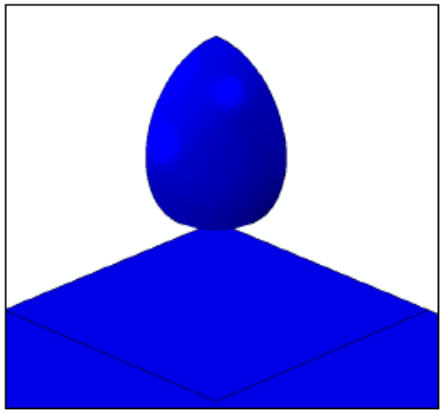

- Plastic deformation Model: Johnson-Cook model
- Initial velocity: 640 m/s (similar to calculated impact velocity for sample made by carrier gas at 300 °C.

Modification to model to address powder roughness and initial oxide layer

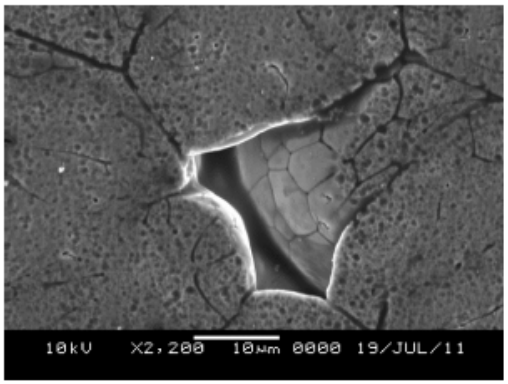

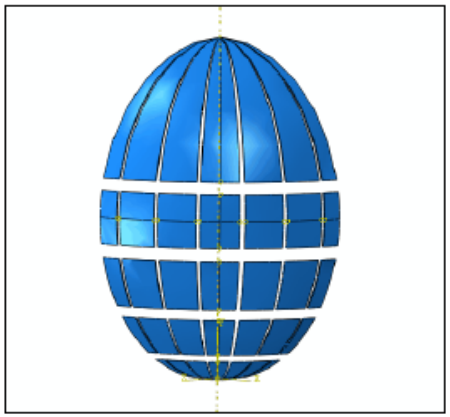

Results of Roughened Impact Models

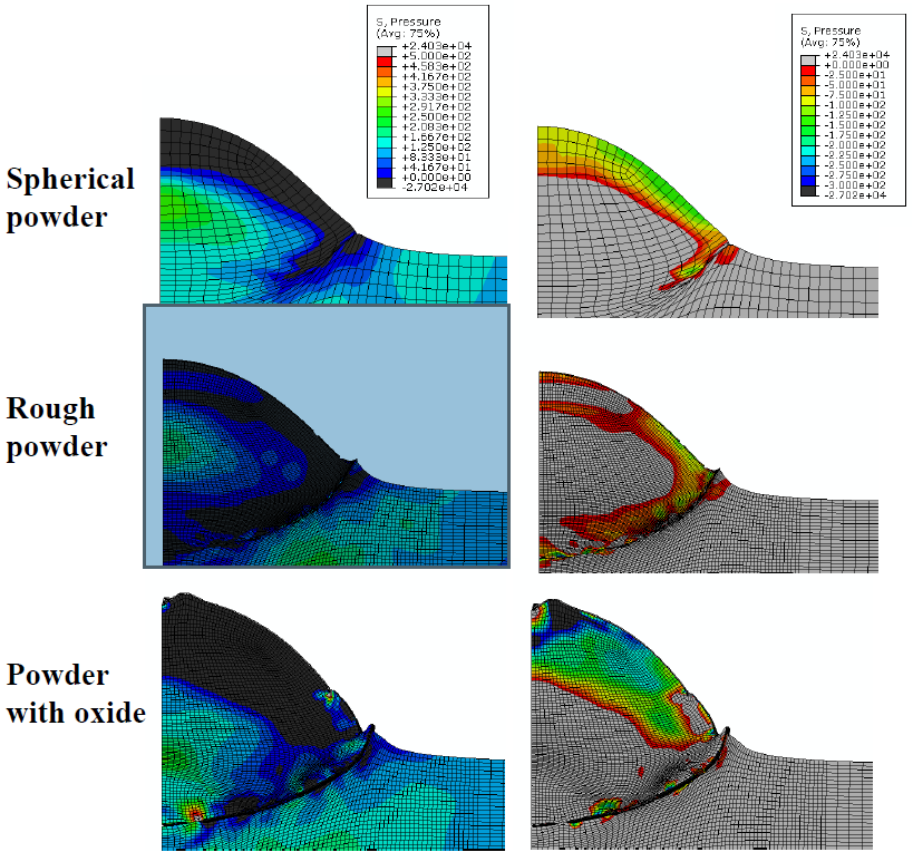

Aluminum etching rate changes for different models

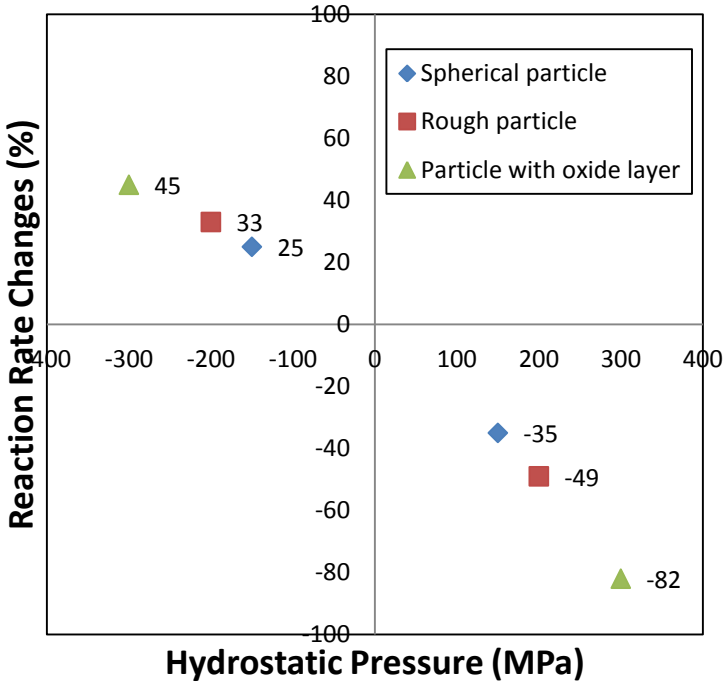

Also important/connected – locations near oxides, high plastic strain, dislocations... brings us to simulations on that scale...

Modeling Note (Nonequilibrium Molecular Dynamics)

Simulation Setup:

Atomic simulation code and computational environment:

- LAMMPS [1] from Sandia National laboratories
- Multi-CPU cluster at NEU

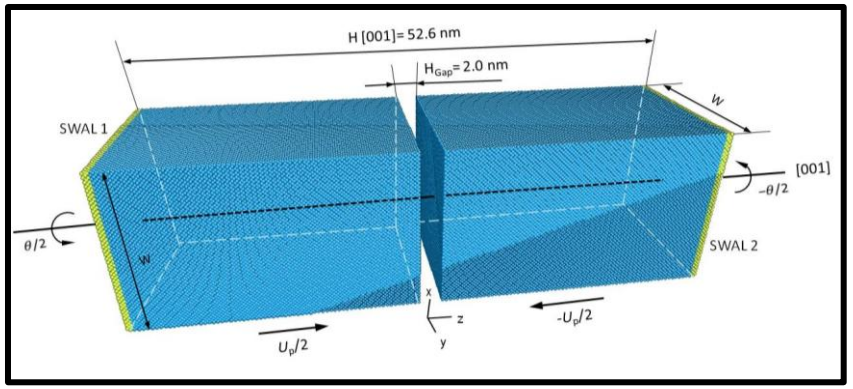

Approximations made at this stage:

- Assume the geometry is atomically flat
- Assume material is chemically pure single crystal

Simulation configuration:

Geometry 1: Commensurate impact on (001) copper surfaces:

- $15 \times 15 \times 50$ nm^3 and 990,000 atoms

Geometry 2: Incommensurate impact on (001) copper surfaces:

- Rotating plates around the z-axis (relative rotation angle 15°, 30° and 45°)
- The systems are on the order of 10^5 atoms

Output:
Transient Atomic positions, velocities

Post process:
temperature, stress distribution, surface energy and work of adhesion

Atomic interaction potential:

- Mishin et al. [2] embedded-atom-method (EAM) potential for copper (many-body pot)

Boundary condition:

- x-and y-directions: periodical boundary condition
- z-direction: specific **S**hock **W**ave **A**bsorbing **L**ayers (SWALs) to remove the reflection wave

[1] Plimpton, S., Fast parallel algorithms for short-range molecular dynamics. Journal of Computational Physics, 1995
[2] Mishin, Y., et al., Structural stability and lattice defects in copper: Ab initio, tight-binding, and embedded-atom calculations. Physical Review B, 2001

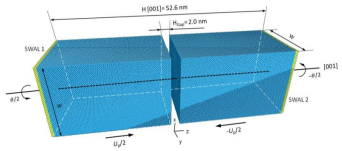

Overall Response

Dislocation Activities

Dislocation nucleation and emission
of impact for u_p = 600 m/s commensurate case
(perfect fcc atoms are removed)

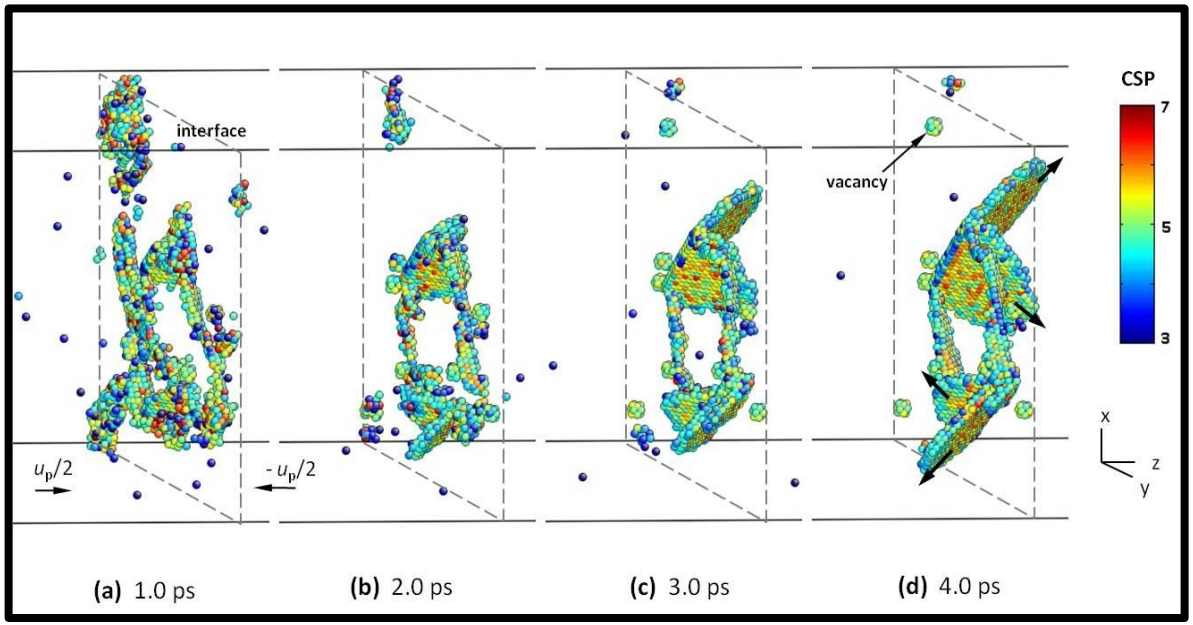

- Severe disordering sites emerge at interface prior to dislocation
- Some of disordered atoms depress and form stable vacancies
- Partial dislocations are nucleated from the remained disordered loop
- Dislocation emission on close packaged surfaces {111}
- For this case only two pairs of active slip planes can be seen

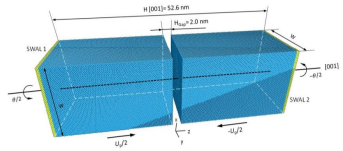

Overall Response

Dislocation Activities

Dislocation nucleation and emission
of impact for u_p = 1200 m/s incommensurate case (θ=15°)

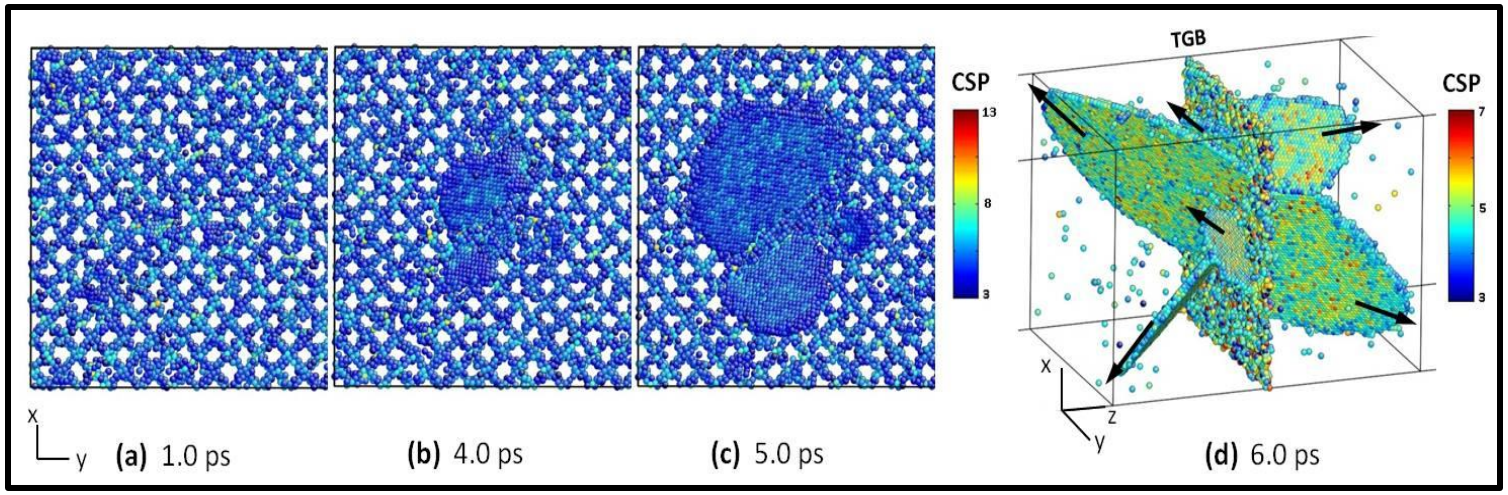

- Twist grain boundary (TGB) are formed prior to dislocation
- Defective atoms emerge and mostly located near the TGB
- Partial dislocations are nucleated from disordered TGB sites into both lattice regions
- Dislocation emission on close packaged surfaces {111}
- For this case, small glides are observed on planes parallel to the main slip planes

Bicrystal model:

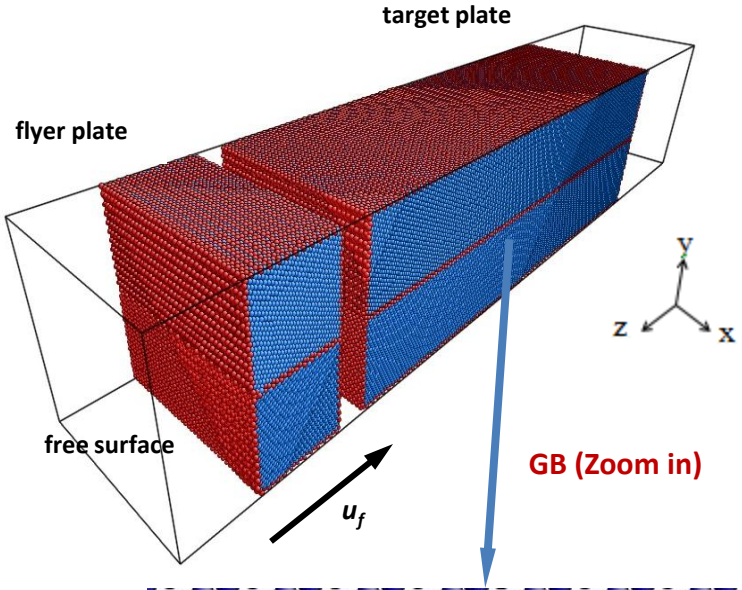

Model description

- material: bicrystal fcc copper
- dimension: 13.74×13.18×6.86 nm^3 (flyer), 13.74×13.18×43.44 nm^3 (targ
- atom amount: 800,000
- interaction potential: Embedded atom method (EAM) [2]
- boundary condition:
  - periodic boundaries perpendicular to ±x directions
  - free surfaces at front and rear surfaces along z direction
  - ∑5 (310) GB tilt along [100] axis
  - flyer plate is assigned a desired atom velocity

Simulation procedure

- use molecular statics to determine bicrystal structure
- thermal equilibrium procedure is the same as single crystal model
- 16ps calculation with impact velocities applied to flyer plate

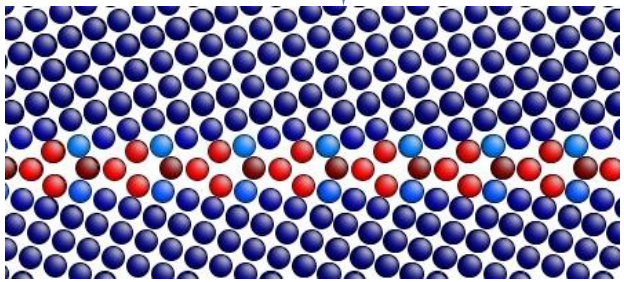

Calculated structure

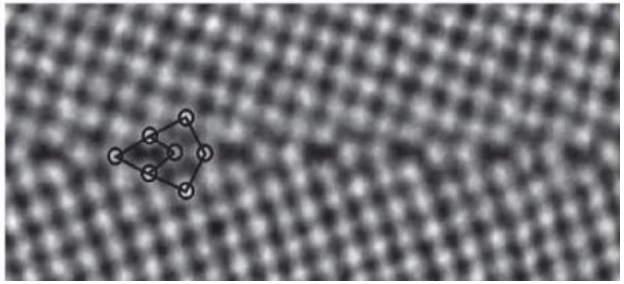

HRTEM images [1]

[1] Duscher, G., et al., Bismuth-induced embrittlement of copper grain boundaries. nature materials, 2004. 3: p. 621-626.

Stress distribution in bicrystal:

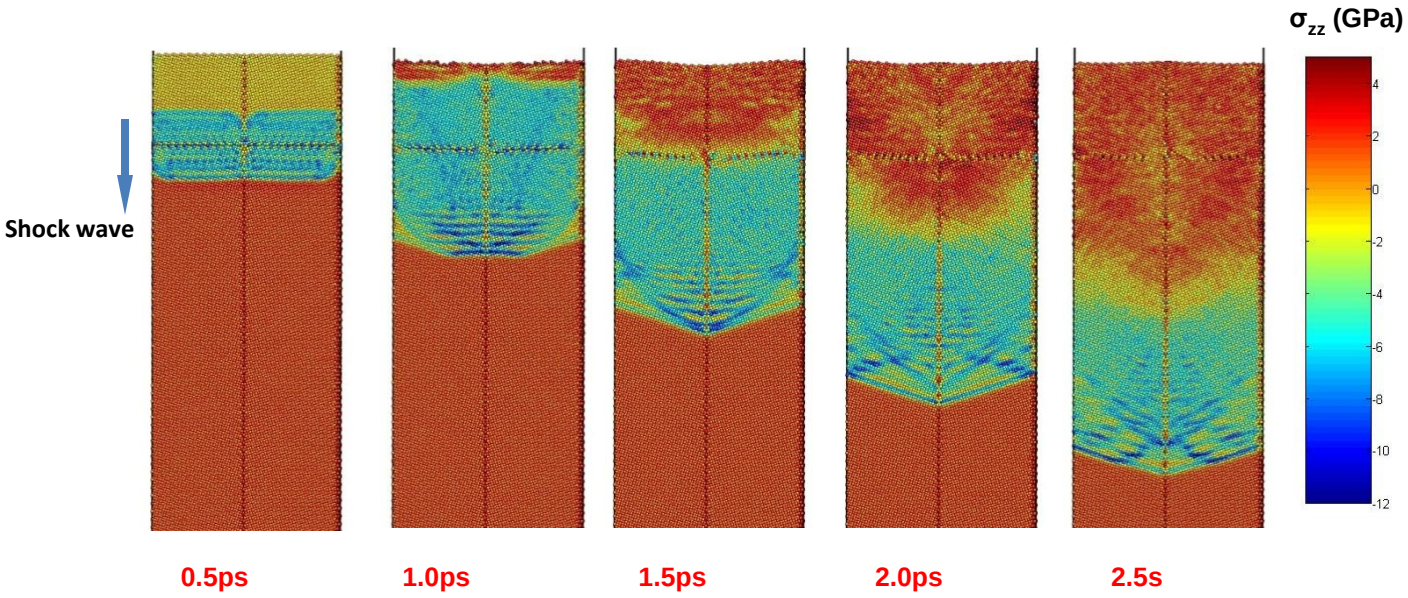

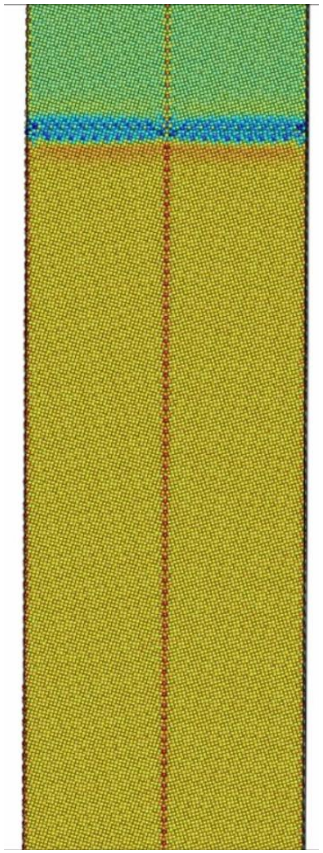

- a planar shock wave around 10GPa is generated at the interface before impact (0.5ps)
- the wave front no longer keeps planar shape as the wave propagates along *z* axis
- atoms near grain boundary preform a higher stress state than other atoms
- stable shock wave front is formed at about 1.5ps after impact, with an angle of 144°

Conclusion

- Impact location:
  - Secondary impact location has bearing on simulation outcome
- Feed rate and cooling time
  - It is shown that it is (more) likely for the particle to reach thermal equilibrium before a second particle hits at the same location.
  - Allowing the initial particle to cool reduces damage
- Temperature:
  - Effects of particle and substrate temperatures are critical
  - Impacting on a heated substrate reduces initial particle damage
- Heterogeneous etch behavior could provide insight into particle bonding
- FEA, MD can provide further insight.

Backup for MD

Temporal evolution of average interface temperature

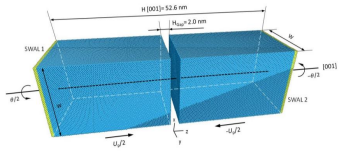

(a) Commensurate impact

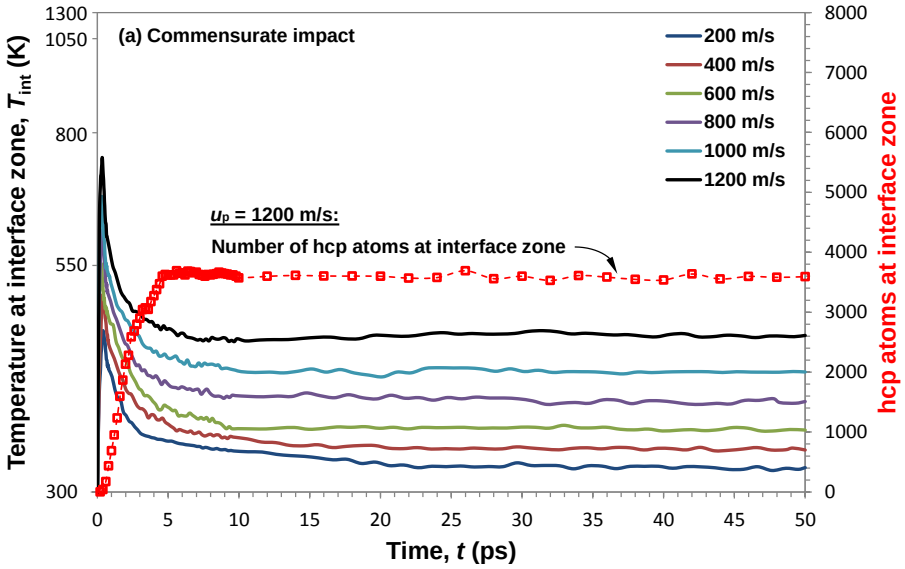

(c) Incommensurate impact with 30 degree rotation

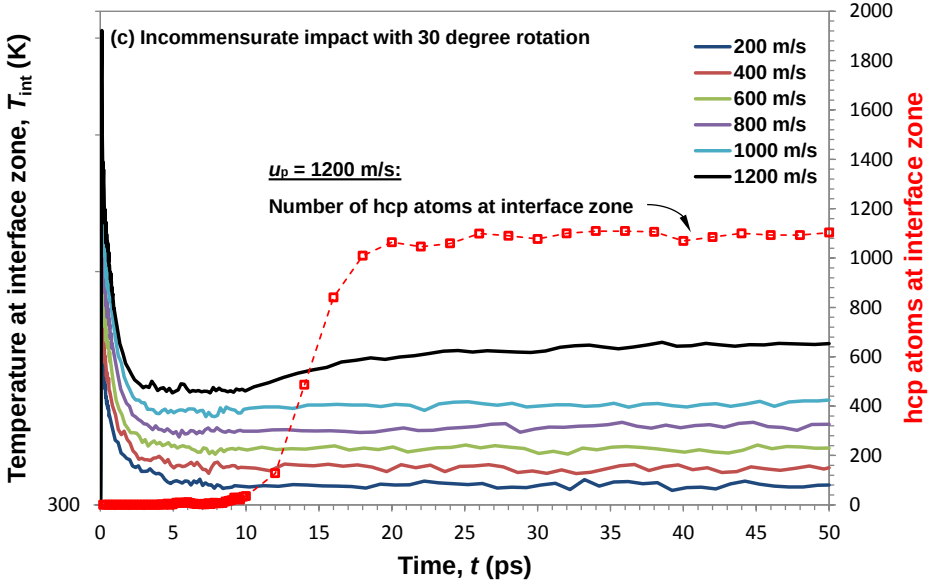

- Initial KE transfer to interface atoms results in a rapid O(0.1 ps) rise to maximum value
- Followed by a relatively slow decay O(5-10 ps) to a steady value
- Temperature decay is associated with redistribution of interface atoms to HCP state
- Impact causes FCC to become disordered indicative of degree of plastic deformation.
- T_{max} always stays well below T_{melt}.

Interface temperature

Max Interface Temperature

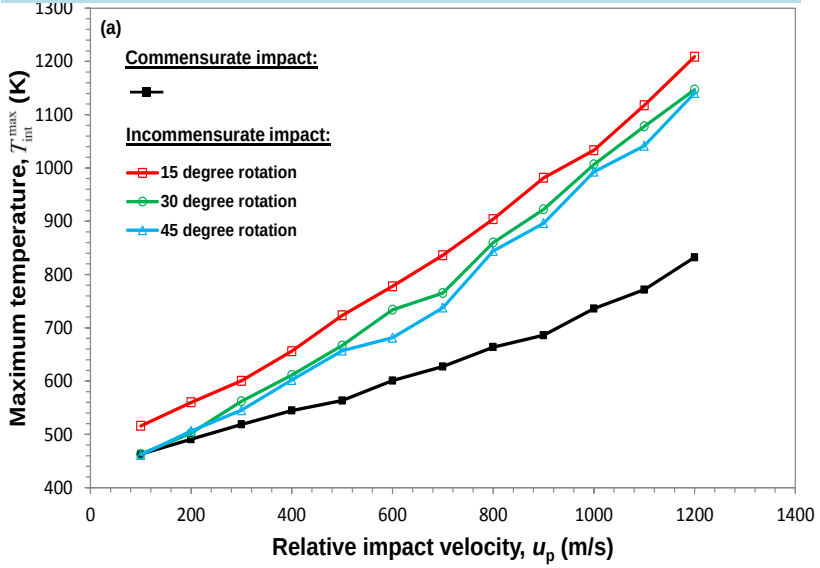

Equilibrium Interface Temperature

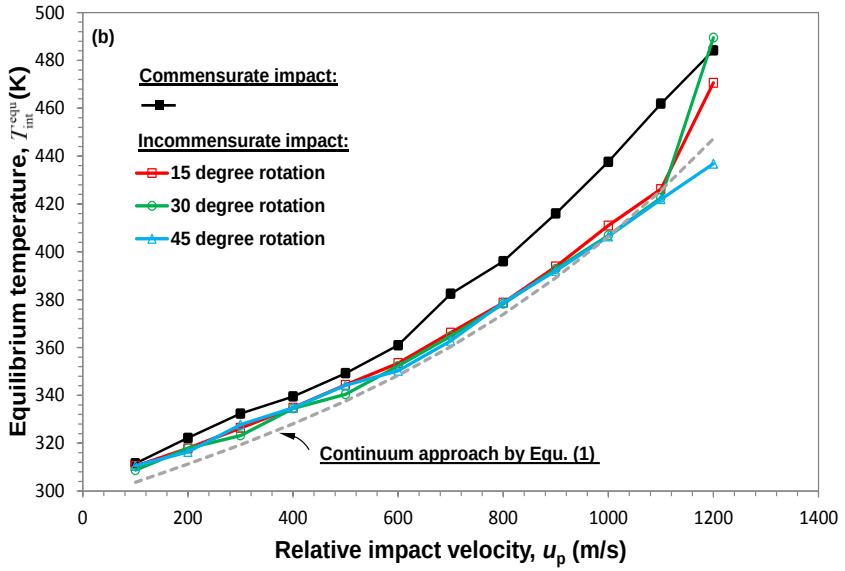

Maximum interface temperature

- increases non-linearly with impact velocity.
- sensitive to interface type.
- following incommensurate impact is always higher

Equilibrium interface temperature

- following 50 ps simulations is same as in bulk.
- increases non-linearly with impact velocity.
- sensitive to interface type.
- following incommensurate impact is almost always lower

Temperature trend curve fit

$$T_i(t) = T_i^{eq} + A\left[ae^{-t/\tau_d} + (1-a)e^{-t/\tau_r} \right]$$

Interfacial energetics

Atomic trajectories yield quantitative measures of non-equilibrium surface energy γ_s^H and work of adhesion W^H that together determine bonding characteristics.

Interface energy (enthalpy): Excess interaction energy of the bicrystal E_t compared to energy of the perfect bulk copper crystal, E_b.

$$\gamma_i^H = \frac{E_t - E_b}{A}$$

E_t: Total energy in the system
E_b: Energy in bulk away from interface r
A: Interface area
$E_{s1}+E_{s2}$: Energy of system after cleaving

Energy (enthalpy) of metallic bonds: obtained by artificially cleaving the interface at z = 0 into two free surfaces. Work done for cleaving give the enthalpy (energy) of metallurgical bonds

$$W^H = \frac{E_{s1} + E_{s2} - E_t}{A}$$

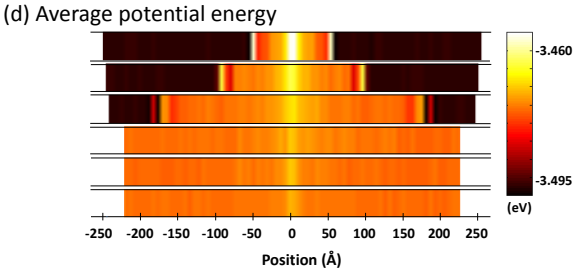

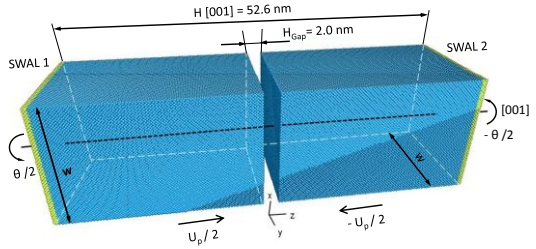

Interfacial energetics

Interface Energy

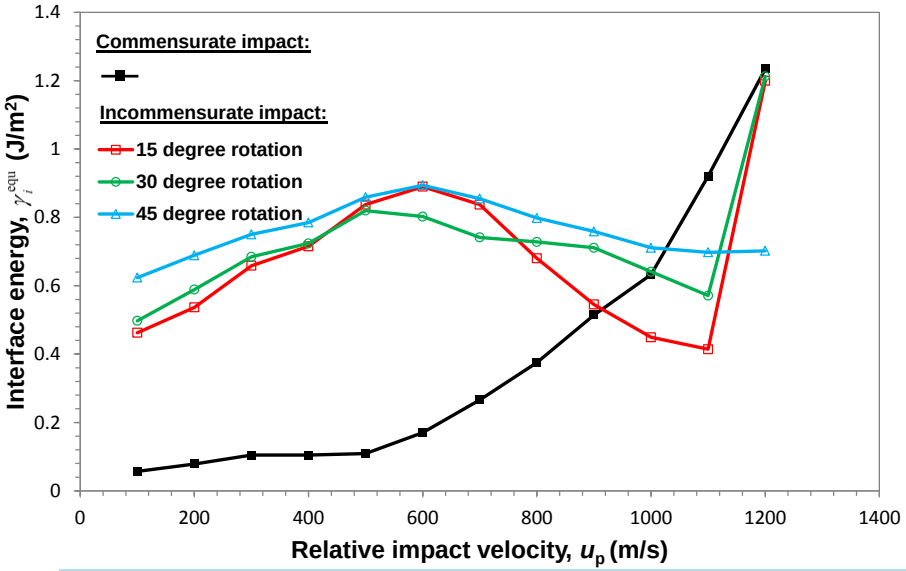

Work of Adhesion

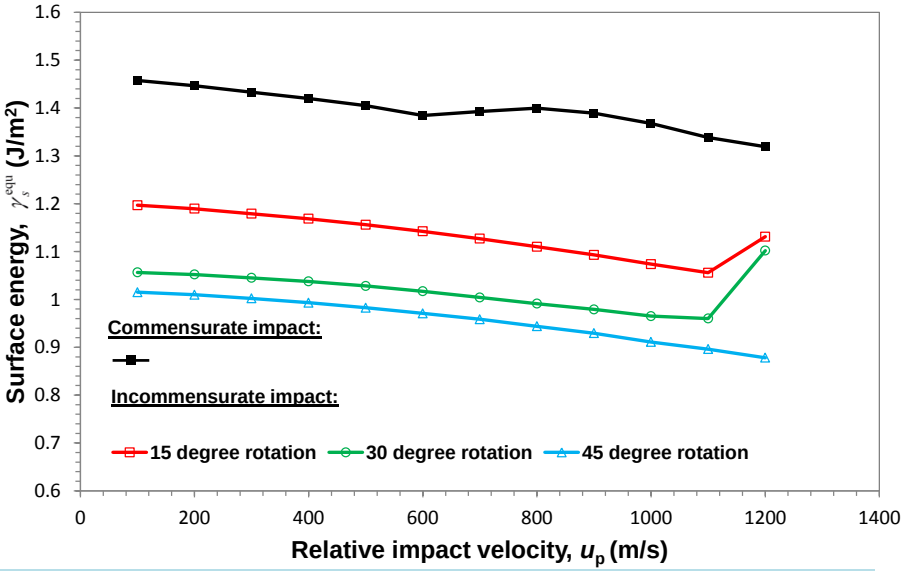

Interface energy

- Quantitative trends at low velocities are close to equilibrium values
  - 0 for commensurate and 0.4 – 0.7 J/m^2 for incommensurate impacts.
- Consistent with grain boundary energies of FCC metals TGB

Work of adhesion (surface energy):

- This represents effects of non-equilibrium energetics & kinetics on metallurgical bond strength
- Strongest bonds are formed with commensurate impact (expected)
- W^H is weakly related to impact velocity but it decreases with u_p.

What did we learn from molecular dynamics?

- Temporal variations in
  - Interface temperature: Interface temperature due to creation of a new interface can contribute a significant amount of temperature rise. Although this would dissipate into the bulk …
  - Work of adhesion is a weak function of impact velocity but a stronger function of orientation
- Plasticity mechanisms due to impact
  - Are responsible for temporal variations of temperature and interface energies

What else can we learn from molecular dynamics?

- Bi-crystal interfaces
- Effects of Initial defects, grain boundaries, nano-scale roughness, oxide content on all of the above …

Information (e.g. T_i, W_i) gained from this study is directly applicable/testable in continuum simulations.

Backup for 100 Particles

Modeling Impact of 100 Al-particles

FEA Model

- Aluminum Particles
- Aluminum Substrate
- Diameter: 31 µm
- Particle Position
  - Randomized X-Z coordinates
- Gas Parameters
  - N_2
  - 3 MPa
  - Inlet Temperature: 573, 673, 773 °K

Gas T (K)	Par V (m/s)	Par T (K)
773	677	601
673	632	524
573	581	448

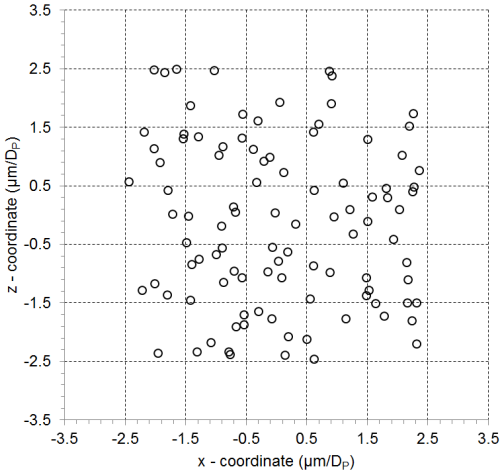

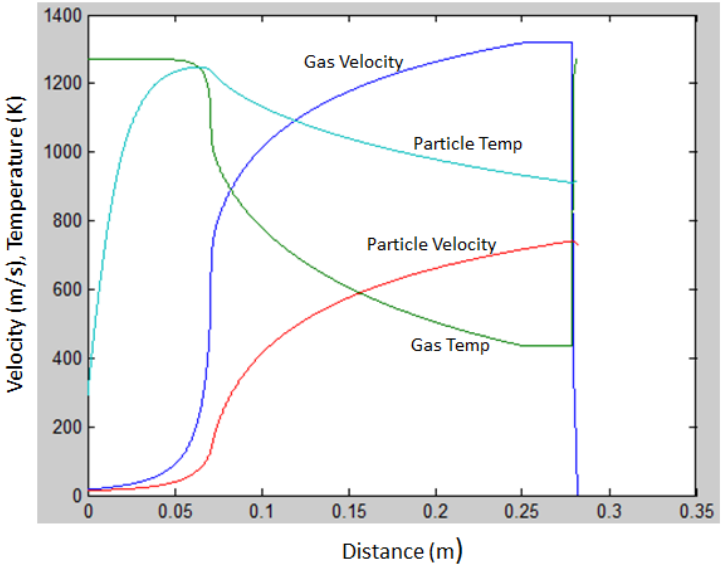

Von Mises and Equivalent Strain Distributions

573 °K

673 °K

773 °K

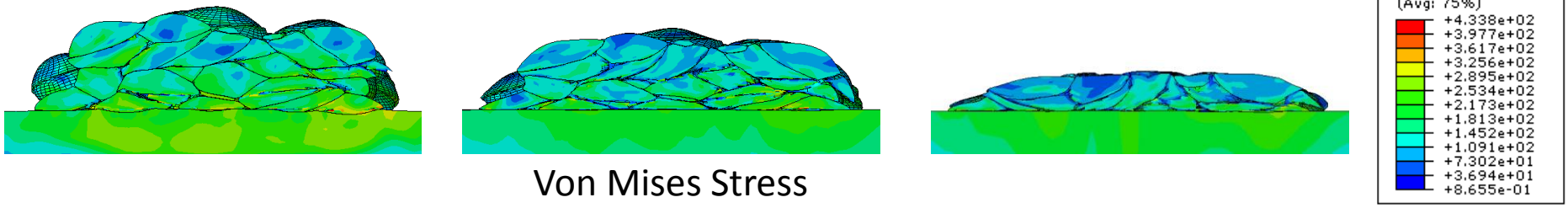

Von Mises Stress

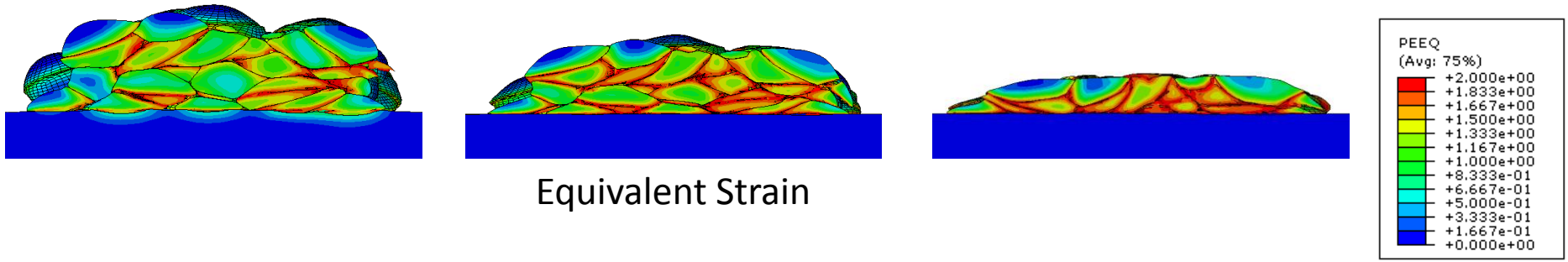

Equivalent Strain

1st and 3rd Principal and Maximum Shear Strain Distributions

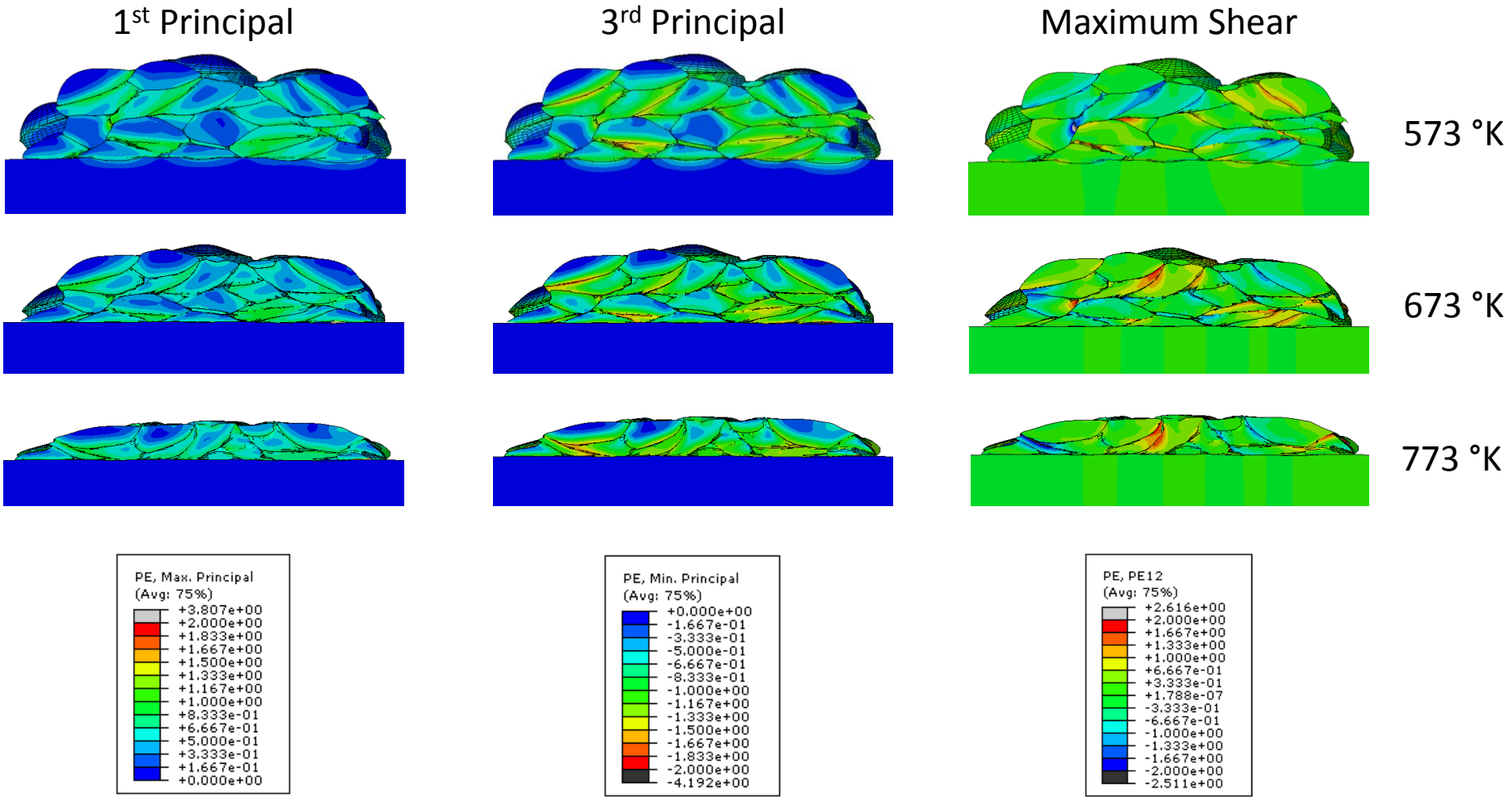

Image processing pipeline: Experimental Method

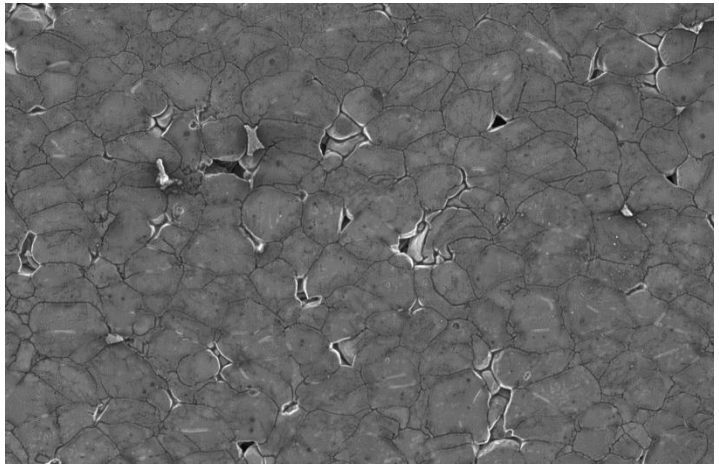

Original SEM

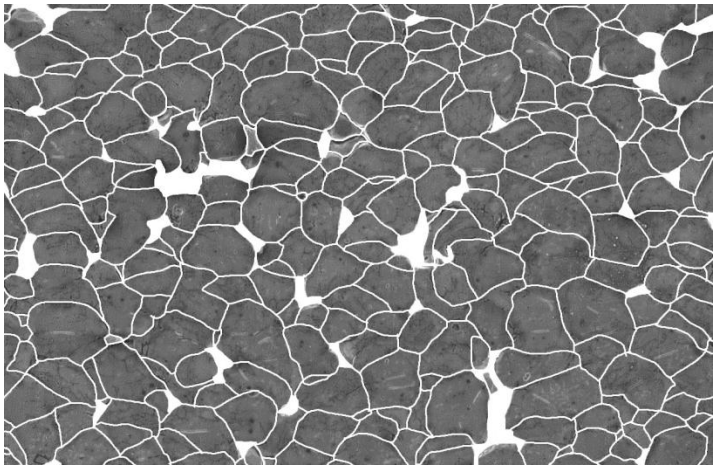

Modified SEM

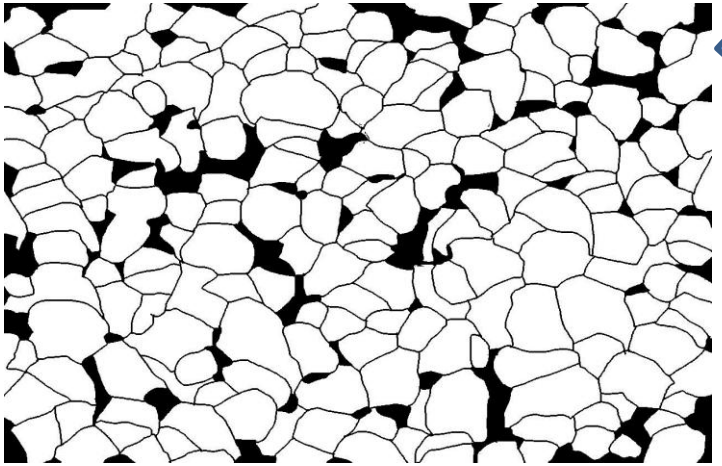

Black and White SEM

SEM Modification

- Boundaries manually drawn
- Voids filled
- Translated to black and white
- Smallest particles withdrawn
  - Eliminates particle fragments
- Three images analyzed
  - 573 K (250x), 673 K (200x), 773 K (200x)

Shape metrics: for SEM Images

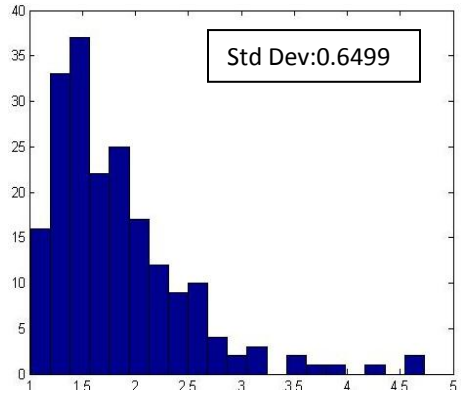

Axis Ratio

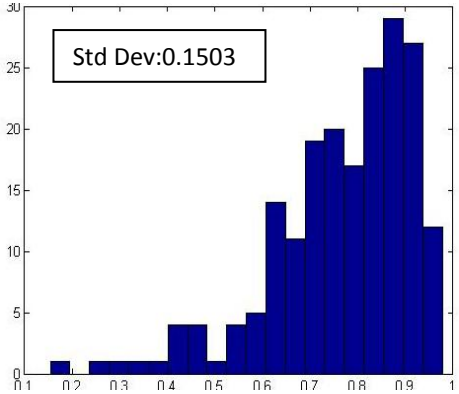

Eccentricity

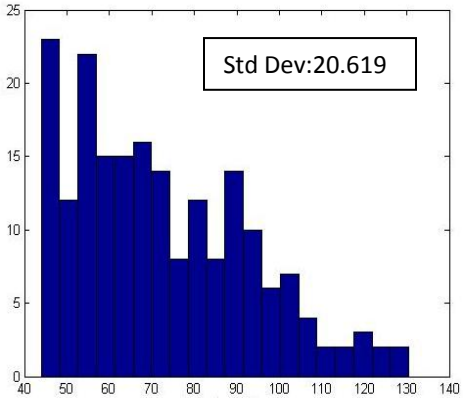

Equivalent Diameter

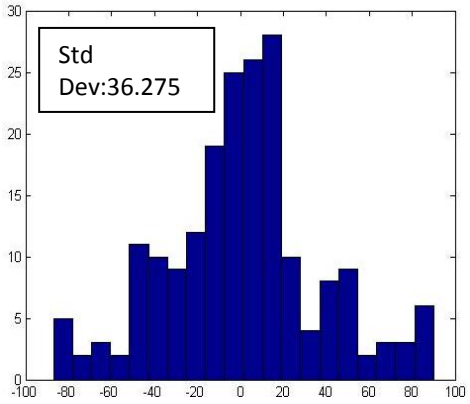

Orientation Angle

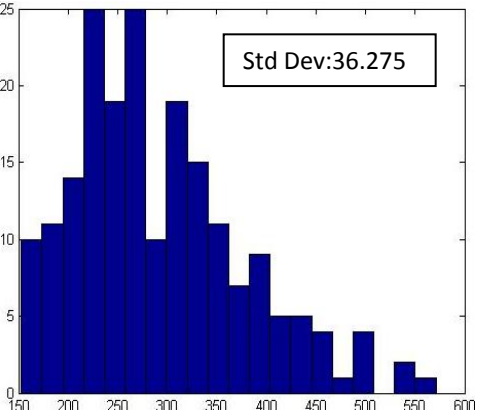

Perimeter

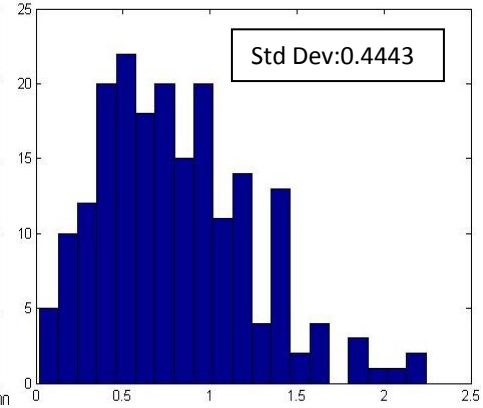

Elongation

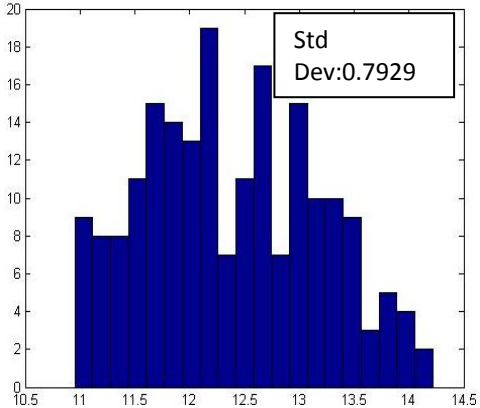

Dispersion

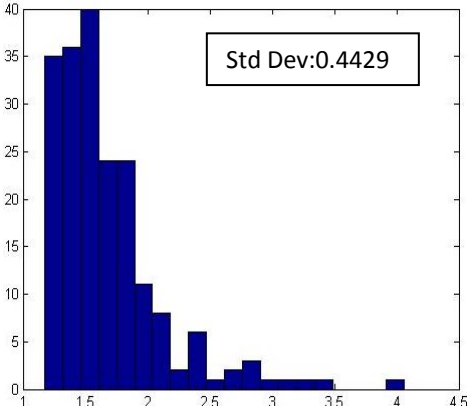

Roundness

Results for SEM image of Al upon Al substrate at 573 K inlet gas temperature